Electronic Supplementary Material (ESI) for Analyst.

ELECTRONIC SUPPLEMENTARY INFORMATION

Polyacrylamide gel electrophoresis of semiconductor quantum dots and their bioconjugates: Materials characterization and physical insights from spectrofluorimetric detection

Hyungki Kim, Tiffany Jeen, Michael V. Tran, W. Russ Algar*

Department of Chemistry, University of British Columbia,
2036 Main Mall, Vancouver, British Columbia, V6T 1Z1, Canada.

* Corresponding author: algar@chem.ubc.ca

Table of Contents

Additional Experimental Details

Ligand exchange with GSH and DHLA

Ligand exchanges with dihydrolipoic acid (DHLA) and glutathione (GSH) were done following previously established protocols.[1]

Synthesis of DHLA-SB

Scheme S1 summarizes the synthesis of the LA-SB ligand, which is the precursor to the final DHLA-SB ligand. The method is based on ref.[2]

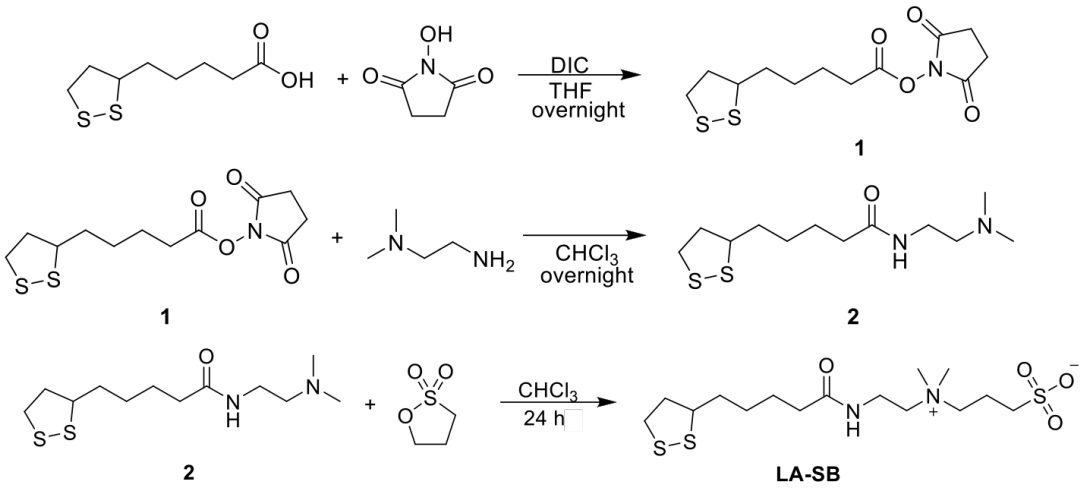

Scheme S1.

Materials

Lipoic acid (LA, ≥99%), *N*,*N*′-diisopropylcarbodiimide (DIC, >98%), *N*-hydroxysuccinimide (NHS, 98%), 1,3-propanesultone (98%), *N*,*N*′-dimethylethylenediamine (95%) were from Sigma-Aldrich (Oakville, ON, Canada).

*Synthesis of lipoic acid-succinimidyl ester (LA-NHS) (**1**)*

Lipoic acid (4.0 g, 19 mmol) and *N*-hydroxysuccinimide (2.9 g, 25 mmol) were dissolved in 25 mL of tetrahydrofuran (THF). *N*,*N*′-Diisopropylcarbodiimide (3.6 mL, 23 mmol) was diluted

into 5 mL of THF and then added dropwise to the reaction mixture. The reaction was stirred overnight at room temperature. A white precipitate formed and was filtered out. The filtrate was concentrated and the crude product was recrystallized with isopropanol. The LA-NHS product was obtained as a yellow powder (5.5 g, 93% yield). ^{13}C NMR ($CDCl_3$, 400 MHz): δ 169.3, 168.5, 56.2, 40.2, 38.6, 34.5, 30.9, 28.4, 25.7, 24.5. ESI-MS (pos, *m/z*): 326.1 $[M+Na]^+$.

*Synthesis of tertiary amine-modified lipoic acid (**2**).*

LA-NHS (3.0 g, 10 mmol) was dissolved in 50 mL of chloroform. *N*,*N*'-dimethylethylene-diamine (2 mL, 18 mmol) was added into the LA-NHS solution dropwise. The reaction was stirred at room temperature overnight. To work-up the reaction, the crude product was first diluted with 30 mL of chloroform, then washed three times with brine. The combined organic layers were dried over Na_2SO_4 (s) and the solvent was evaporated to give a yellow oil (2.43 g, 89% yield). ^{1}H NMR ($CDCl_3$, 400 MHz): δ 6.02 (br, s, 1H), 3.56 (m, 1H), 3.32 (q, 2H), 3.07-3.20 (m, 2H), 2.38-2.49 (m, 3H), 2.16-2.22 (m, 8H), 1.86-1.94 (m, 1H), 1.62-1.72(m, 4H), 1.39-1.50 (m, 2H). ^{13}C NMR ($CDCl_3$, 400 MHz): δ 172.9, 57.9, 56.6, 45.3, 40.4, 38.6, 36.8, 36.5, 34.8, 29.1, 25.6. ESI-MS (pos; *m/z*): 277.3 $[M+H]^+$, 295.4 $[M+Na]^+$.

Synthesis of LA-SB

1,3-propanesultone (2.4 g, 20 mmol) was dissolved in 10 mL of anhydrous chloroform and compound **2** (1.8 g, 6.5 mmol) was added to the solution. The reaction was stirred for 24 h at room temperature. The crude product precipitated out of the solution and was isolated by filtration. The precipitate was washed with chloroform and the product was obtained as a chalky yellow solid (1.9 g, 75 % yield). ^{1}H NMR (D_2O, 400 MHz): δ 7.68 (br, s, 1H), 3.68-3.74 (m, 3H), 3.48-3.56 (m, 4H), 3.18-3.27 (m, 8H), 2.98-3.01 (t, 2H), 2.46-2.54 (m, 1H), 2.23-2.32 (m, 4H), 1.97- 2.05 (m, 1H), 1.58-1.80 (m, 4H), 1.39-1.46 (m, 2H). ESI-MS (pos, *m/z*): 399.1 $[M+H]^+$.

Ligand exchange with DHLA-SB

LA-SB (30 mg, 75.2 μmol) was dissolved in 100 μL deionized (DI) water in a 1.7 mL microcentrifuge tube and tris(2-carboxyethyl)phosphine (TCEP; 50 mg, 0.174 mmol) was added to the solution. The mixture was vortexed and set aside for 30 min at room temperature. The reaction mixture was then divided between two microcentrifuge tubes and 1.1 mL of acetone was added to each tube. The solutions were vortexed until cloudy and centrifuged at 17 000 rcf for 5 min. The reduced DHLA-SB ligands remained at the bottom as a clear liquid. After the supernatant was discarded, the two volumes of ligand were combined and diluted in 100 μL of DI water. Next, 200 μL of tetramethylammonium hydroxide solution (TMAH; 25% w/w in methanol) was added to the ligand solution. In a new microcentrifuge tube, 2.7 μL of 74 μM QD650 in toluene was combined with 1 mL of ethanol. The QDs were pelleted by centrifugation (2000 rcf), the supernatant discarded, and the QDs redispersed in 100 μL of chloroform. The resulting solution of QDs was added into the ligand solution and vortexed. The solution was then incubated at 60 °C for 15 min. Borate buffer (50 mM, pH 9; 100 μL) was then added to the mixture and the reaction was further incubated at 60 °C overnight. After the reaction had cooled to room temperature, the aqueous layer was transferred to a new tube. Ethanol (~600 μL) was used to help pellet the QDs by centrifugation and the supernatant was discarded. The QDs were redispersed in 100 μL of borate buffer (50 mM, pH 9). This process of precipitation, removal of the supernatant, and redispersion was repeated three more times to remove excess ligands. After the final wash, the QDs were redispersed in 300 μL of borate buffer.

Synthesis HDA-PMA and coating of QDs

To prepare HDA-PMA, 10 mg of poly(isobutylene-*alt*-maleic anhydride) (PMA) and ~29 equiv. (per polymer chain) of hexadecylamine (HDA) were mixed in 1.5 mL THF and did not fully dissolve. The suspension was incubated at 60 °C for 6 h, which produced a clear solution. This solution was then dried under vacuum and the resulting white solid was dissolved in 800 μL of chloroform. Hydrophobic CdSe/ZnS QDs in toluene (33 μL, 74 μM) were then added. The mixture was left at room temperature in the dark overnight, then dried under vacuum. The residue was dispersed in borate buffer (pH 12, 90 mM) under sonication for 30 min. The

resulting solution was purified with a spin filter (Nanosep 10k omega membrane; Pall Corporation, Ann Arbor, MI, USA) at 4800 rcf for 10 min. The QDs were washed three times with borate buffer (pH 8.5, 50 mM) using the spin filter and finally suspended in borate buffer. The HDA-PMA-QD solution was then filtered through 0.22 μm membrane (Millex-GP, Merck Millipore Ltd., Tullagreen, Carrigtwohill, Co. Cork, Ireland). The filtered QD solution was concentrated under vacuum and stored at 4 °C until needed.

Synthesis API-PMA and coating QDs

To prepare API-PMA, 10 mg of PMA and ~29 equiv. (per polymer chain) of 1-(3-aminopropyl)imidazole (API) were added to 900 μL of DMSO. The mixture was incubated at 60 °C to produce a clear solution, which was then dried under vacuum. The white solid was dissolved in 50 μL DMSO, then added to hydrophobic QDs in chloroform (3 μM, 800 μL). TMAH (300 μL) and borate buffer (200 μL; pH 12, 90 mM) were added and the mixture was left at room temperature overnight, in the dark. The bottom organic layer was discarded and 1 mL of ethanol was added the remaining aqueous layer with QDs. This mixture was vortexed and then centrifuged for 5 min at 17 000 rcf. A pellet of QDs formed while some QDs remained in the supernatant. The pellet was discarded and the supernatant was collected and then dried under vacuum. The QD residue was partially dissolved in borate buffer (pH 8.5, 50 mM), the aqueous solution collected and the insoluble portion of the residue discarded. The aqueous solution of QDs was stored at 4 °C until needed. Note: This procedure was satisfactory for the CGE experiments; however, we recommend better optimized workup and purification steps for most other applications.

Agarose slab gel electrophoresis

Agarose slab gels (1.5% w/v) were prepared with 1X Tris-borate (TB) buffer (89 mM; pH 8.3). Samples of QDs (8 μL, 0.1–1.0 μM) were mixed with 2 μL of 20% v/v glycerol (aq) solution, then vortexed. Aliquots (7 μL) were then transferred into the wells of the gel, which was run in 1X Tris-borate TB buffer for 30 min at a field strength of 7.4 V/cm. Gels were imaged under

long-wave UV light (365 nm) with digital camera and UV-blocking filter. PL intensity profiles for the gel were generated in ImageJ (National Institutes of Health, Bethesda, MD, USA).

Absorbance and PL emission measurements of QDs in bulk solution

Absorption and photoluminescence (PL) measurements were made in 96-well plates with a Tecan infinite M1000 Pro Plate Reader (Tecan Ltd., Morrisville, NC). The step size for absorbance measurements was 2 nm. For PL measurements, the excitation and emission monochromator bandwidths were 5 nm and the step size was 2 nm.

Analysis of electropherogram data

As noted in the main text, fluorescein was added to samples of QDs as an internal standard. The migration time (abscissa) for each run was adjusted to align the electropherogram peak of the fluorescein between replicates. Electropherogram peak full-width-at-half-maxima (FWHM) were calculated as $T_{0.5}$–$L_{0.5}$, where $T_{0.5}$ and $L_{0.5}$ are the times for the data points on the trailing and leading sides of the peak that have PL intensities of one-half the peak maximum. Peak asymmetries were calculated as $T_{0.1}/L_{0.1}$, where $T_{0.1}$ is the distance (in units of time) between the peak maximum and the data point with one-tenth of the peak intensity on the trailing side of the peak, and $L_{0.1}$ is the analogous measurement on the leading side of the peak.

To determine the peak PL emission wavelengths at each time point across an electropherogram peak, each measured spectrum was smoothed with a moving average, the maximum PL emission intensity determined, and the corresponding wavelength recorded.

Background in PL emission measurements

Electropherograms were measured under parameters where the background was approximately flat. In many experiments, the background was negligible. When not negligible, the average value of the background was subtracted from PL intensity measurements prior to normalization and further data analysis.

Fitting Ferguson analysis data for effective radii and zeta potentials

Eqns. S1-S2 are the basis of a Ferguson analysis with QDs, where the mobility, M, was calculated as the quotient of the migration velocity (cm s^{-1}) over the field strength (V cm^{-1}), M_0 was the extrapolated free mobility of the particle in the absence of the gel, K_R was the retardation factor, and T was the gel concentration.[3, 4] The terms a and b in Eqn. 2 are empirical constants and R is the effective radius of the QD.

$$\log M = \log M_0 - K_R T \tag{S1}$$

$$\sqrt{K_R} = aR + b \tag{S2}$$

We have previously analyzed QDs by Ferguson analysis with agarose gels and gold nanoparticles as size standards.[5, 6] For mobilities in units of cm^2 s^{-1} V^{-1}, and R in units of nm, the values of a and b were 0.011 and 0.26, respectively.[6] These values served as initial guesses for a and b for the PAG gels. The Ferguson plots for GSH-QD650, DHLA-SB-QD650, API-PMA-QD650, and HDA-PMA-QD650 were then fit with a combination of global (a, b), local (R), and predetermined ($\log M_0$, from simple linear regression) variables. Levenberg-Marquardt (LM) fitting was run several times with different initial guesses for R to estimate the range of values for a, b, and R obtained from fits. Next, Monte Carlo fitting was run twelve times for more than one million iterations with a search range defined for a and b that bounded the variability seen in repeated LM fitting. The high and low results for each parameter were thrown out and the average values plus/minus the standard deviations were reported as the values of R. The average values of a and b for PAG were 0.016 ± 0.002 and 0.32 ± 0.02, respectively.

Zeta potentials were calculated *via* Eqn. S3, a rearrangement of Eqn. 4 from the main text, where ζ is the particle zeta potential, η is the viscosity of the medium, ε_r is its relative permittivity, and ε_0 is the vacuum permittivity.

$$\zeta = \frac{3\eta M_0}{2\varepsilon_r \varepsilon_0} \tag{S3}$$

QD core size and peak PL emission wavelength

The bandgap energy of QD, E_{QD}, can be estimated from the Brus equation, Eqn. S4, where E_g is the bulk bandgap energy (2.80×10^{-19} J for CdSe), R is the radius of the QD core, m_e and m_h are the effective masses of an electron and hole in the semiconductor ($0.13m_o$ and $0.45\ m_o$ for CdSe, with $m_o = 9.11\times10^{-31}$ kg), e is the elementary charge, ε is the relative dielectric constant of the semiconductor (5.8 for CdSe), and ε_0 is the vacuum permittivity.[7]

$$E_{QD} \approx E_g + \frac{\hbar^2\pi^2}{2R^2}\left(\frac{1}{m_e}+\frac{1}{m_h}\right) - \frac{1.8e^2}{4\pi\varepsilon\varepsilon_0 R} \qquad \text{(S4)}$$

Although there is small wavelength offset between the first exciton peak and the wavelength of maximum PL emission for a QD, we take the value of E_{QD} to correspond to the emission maximum, which was calculated for a series of values of R to generate the plot in Fig. S10A (*vide infra*). To complete this plot, we calculated the electrophoretic mobility, M, as a function of R based on the Ferguson plot parameters. The value of $1/M$, which is directly proportional to the migration time, was found to scale linearly with R over the range of values relevant to Fig. S10A.

Analysis of QDs by CE

Capillary electrophoresis (CE) experiments were performed with an Agilent 7100 CE system (Agilent Technologies, Saint Laurent, QC, Canada) equipped with a diode array detector (DAD) for UV-visible absorption and a fused silica capillary with an inner diameter of 50 μm. The effective length of the capillary was 52 cm (total length 5 m). The applied potential was 25 kV with a current of 60 μA.

For preconditioning, the capillary was rinsed in sequence with methanol, 0.1 M NaOH, water, and borate buffer (20 mM, pH 9.3) for 5 min each. The capillary was rinsed again with borate buffer for 4 min prior to each injection (5 s injection time, 50 mbar injection pressure). Following each run, the capillary was post-conditioned by rinsing with 0.1 M NaOH and then water for 3 min each. The pressure was 1 bar during rinses and the CE runs. The temperature was

maintained at 20 °C. Borate buffer (20 mM, pH 9.3) was used for the CE runs. QDs were injected at the anodic side of the capillary and traveled towards the cathode with the electroosmotic flow. Data was recorded at multiple wavelengths, but the electropherograms were plotted for the signal at 240 nm. All CE runs were performed in triplicate.

For DHLA-SB-, API-PMA- and HDA-PMA-QD650, carboxyfluorescein (FAM) was used as an internal standard instead of fluorescein to avoid co-migration problems. FAM succinimidyl ester (NHS), 6-isomer (Lumiprobe, Hallandale Beach, FL, USA) was stored in borate buffer (100 mM, pH 9.2) for > 7 days at 4 °C to prepare FAM by hydrolysis.

Analysis of gold nanoparticles by PAGE

Gold nanoparticles (Au NPs) coated with citrate (5 nm and 10 nm diameter) were obtained from Cytodiagnostics (Burlington, ON, Canada). GSH- and DHLA-coated Au NPs were prepared via ligand exchange. Minor modifications were made to the ligand exchange procedure used for GSH- and DHLA-QDs. GSH or lipoic acid (260 μmol) was mixed with either 5 nm Au NPs (100 pmol) or 10 nm Au NPs (10 pmol). GSH-Au NPs were incubated at room temperature for 3 h and DHLA-Au NPs were incubated at 70 °C overnight. Afterward, the Au NPs were centrifuged and the pellets washed with borate buffer (50 mM, pH 9.2). This process was repeated two more times. The washed Au NPs were concentrated under vacuum prior to further analysis.

Characterization of the Au NPs by “stubby” capillary PAGE was analogous to that of the QDs except for a change in microscope configuration, which is illustrated in Fig. S1. The main difference is that the blue excitation light used to interrogate QD PL was replaced with white light (a blue LED with broadband phosphor emission) to interrogate the optical extinction of the Au NPs. Absorption and scattering of this light by Au NPs passing through the imaging field reduced the amount of light transmitted to the spectrometer.

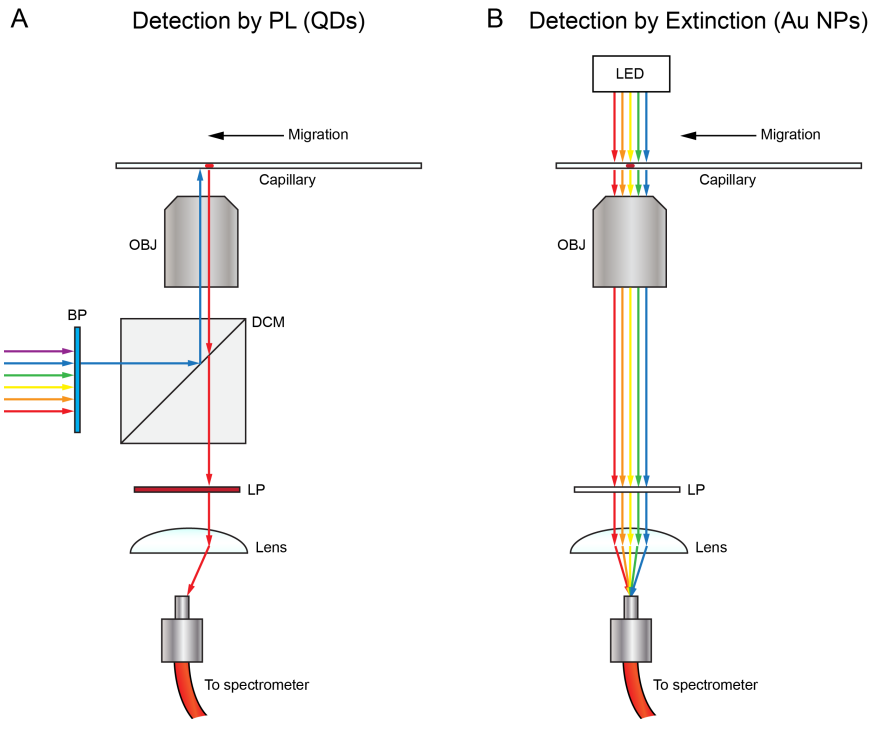

Fig. S1. Simplified schematics of the microscope optical configurations for **(A)** PL-based detection of QDs and **(B)** extinction-based detection of Au NPs.

Separation of fluorescent dye-labeled proteins

Bovine serum albumin (BSA) was obtained from Amresco (Solon, OH, USA). Trypsin inhibitor from *Glycine max* (Soybean) (abbreviated as STI), fluorescein isothiocyanate isomer 1 (FITC) and rhodamine B isothiocyanate (RITC) were acquired from Sigma-Aldrich (Oakville, ON, Canada). An identical procedure was used to prepare BSA-FITC, BSA-RITC, and STI-FITC.

Protein solution (150 µM) and dye solution (2.5 mM) were prepared in borate buffer (100 mM, pH 9.2). Molar equivalents of protein and dye solution were mixed in the dark for 2 h. To remove unreacted FITC, the reaction mixture was dialyzed using 2000 MWCO Slide-A-Lyzer Dialysis Cassette (Thermo Scientific, Rockford, IL, USA) over two days against ~1 L of water at room temperature with one water change. The labeling ratio was ~1:9 for FITC:BSA, ~1:1 for RITC:BSA, and ~1:3 for FITC:STI. The "stubby" capillary PAGE method with the proteins was analogous to the method with QDs except that the PAG density was 7.5% w/w.

Additional Results and Discussion

Absorption and PL emission spectra of QDs

Fig. S2 shows the absorption and PL emission spectra for the QD520, QD570, QD600, and QD650. The spectra were measured for the QDs coated with GSH ligands. Spectra were also measured for QDs coated with DHLA, DHLA-SB, API-PMA, and HDA-PMA but are not shown. The spectra were the same except for small shifts in the peak PL emission wavelength between different coatings.

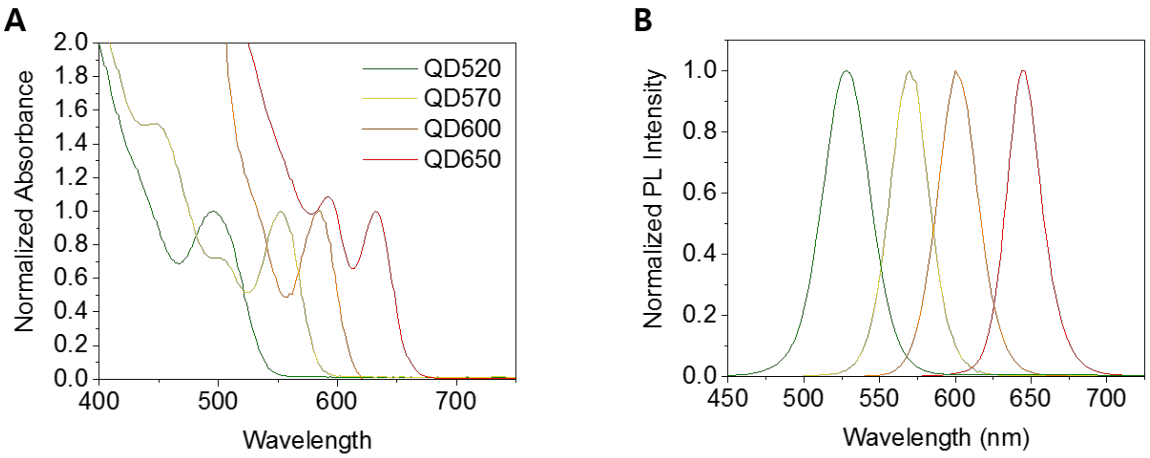

Fig. S2. (A) Absorption and **(B)** PL emission spectra of the QDs.

TEM images of QDs

Fig. S3 shows transmission electron microscope (TEM) images of the QD520, QD570, QD600, and QD650. Nanocrystal sizes were estimated from the measurement of 50 individual nanocrystals in TEM images.

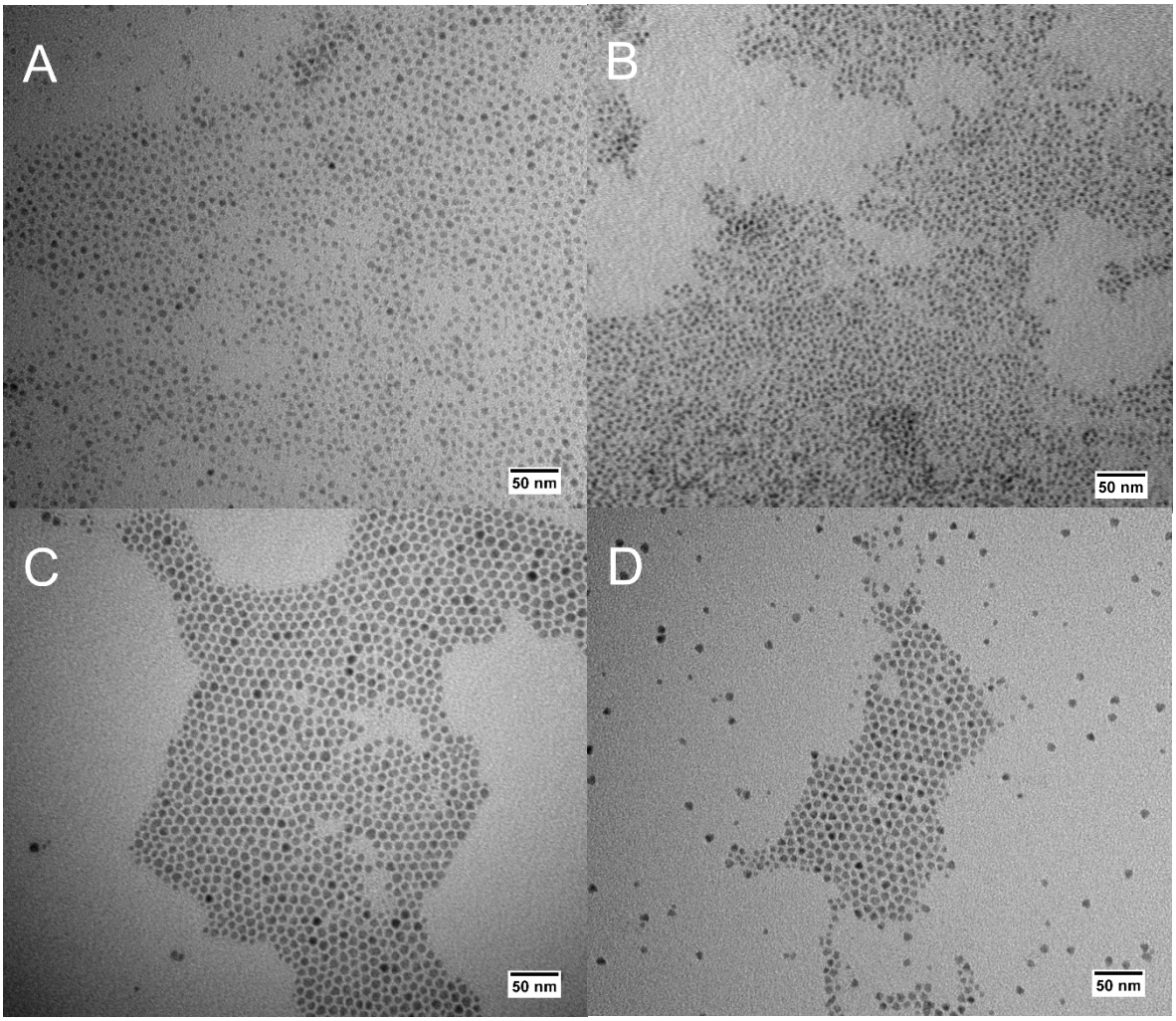

Fig. S3. Representative TEM images of **(A)** QD520, **(B)** QD570, **(C)** QD600, and **(D)** QD650.

Electropherograms and peak parameters

Tables S1 and S2 collect peak parameters for several of the experiments in the main text, including Figs. 3, 5, and 6.

Table S1. Electropherogram peak parameters for X-QD650 at different PAG densities. [a]

X	*GSH*	*DHLA*	*DHLA-SB*	*API-PMA*	*HDA-PMA 1*	*HDA-PMA 2* [d]
Adjusted migration time of QD (min) [b]						
3.0%	1.83 ± 0.04	2.03 ±0.03	7.21 ± 0.08	4.4 ± 0.1	4.94 ± 0.05	5.7 ± 0.5, 7.4 ± 0.5,
3.5%	3.64 ± 0.03	nd	8.0 ± 0.1	5.5 ± 0.2	nd	9.1 ± 0.6, 12.1 ± 0.7
4.0%	6.1 ± 0.2	nd	12.3 ± 0.2	8.7 ± 0.3	nd	15 ± 1, 21 ± 3
5.0%	8.3 ± 0.3	nd	15.5 ± 0.4	14.3 ± 0.2	nd	46 ± 4, na
6.0%	15.6 ± 0.3	nd	28 ± 1	26.1 ± 0.1	nd	na, na
Peak FWHM (min)						
3.0%	0.57 ± 0.02	0.58 ± 0.02	1.4 ± 0.2	1.9 ± 0.3	1.83 ± 0.03	na
3.5%	1.31 ± 0.02	nd	1.78 ± 0.04	2.6 ± 0.1	nd	na
4.0%	2.53 ± 0.06	nd	2.9 ± 0.4	3.9 ± 0.9	nd	na
5.0%	3.7 ± 0.2	nd	2.7 ± 0.3	5.6 ± 0.2	nd	na
6.0%	6.1 ± 0.5	nd	8 ± 3	13.7 ± 0.3	nd	na
Peak asymmetry						
3.0%	2.0 ± 0.1	1.24 ± 0.01	1.7 ± 0.2	2.5 ± 0.2	13 ± 1	na
3.5%	2.5 ± 0.2	nd	1.7 ± 0.2	nd [c]	nd	na
4.0%	3.0 ± 0.1	nd	0.9 ± 0.3	nd [c]	nd	na
5.0%	3.2 ± 0.3	nd	3 ± 1	2.1 ± 0.7	nd	na
6.0%	2.19 ± 0.03	nd	2 ± 1	1.9 ± 0.2	nd	na

[a] All values are ± 1 standard deviation for a minimum of three replicates. nd = not determined; na = not applicable. [b] The adjusted migration time was calculated as the difference between electropherogram peaks for the QD and fluorescein. [c] The appearance of the second peak interfered with this calculation. [d] The first value corresponds to the first local maximum in the electropherogram; the second value corresponds to the second local maximum.

Table S2. Electropherogram peak parameters for QD600-[peptide]$_N$ run on 3.0% PAG.

N	0	2	4	8	16	32
Adjusted migration time (min)	2.08 ± 0.05	2.15 ± 0.7	2.4 ± 0.5	3 ± 1	4 ± 1	6 ± 1
Peak FWHM (min)	1.4 ± 0.2	1.3 ± 0.2	1.4 ± 0.4	1.6 ± 0.3	1.7 ± 0.2	2.0 ± 0.1
Peak Asymmetry	4.3 ± 0.9	3.4 ± 0.8	2.1 ± 0.5	1.6 ± 0.1	1.5 ± 0.1	1.27 ± 0.1

Figs. S4–S6 show electropherograms that were not shown in the main text and are representative data for the Ferguson analysis in Fig. 5D. The data for GSH-QD650 can be found in Fig. 3.

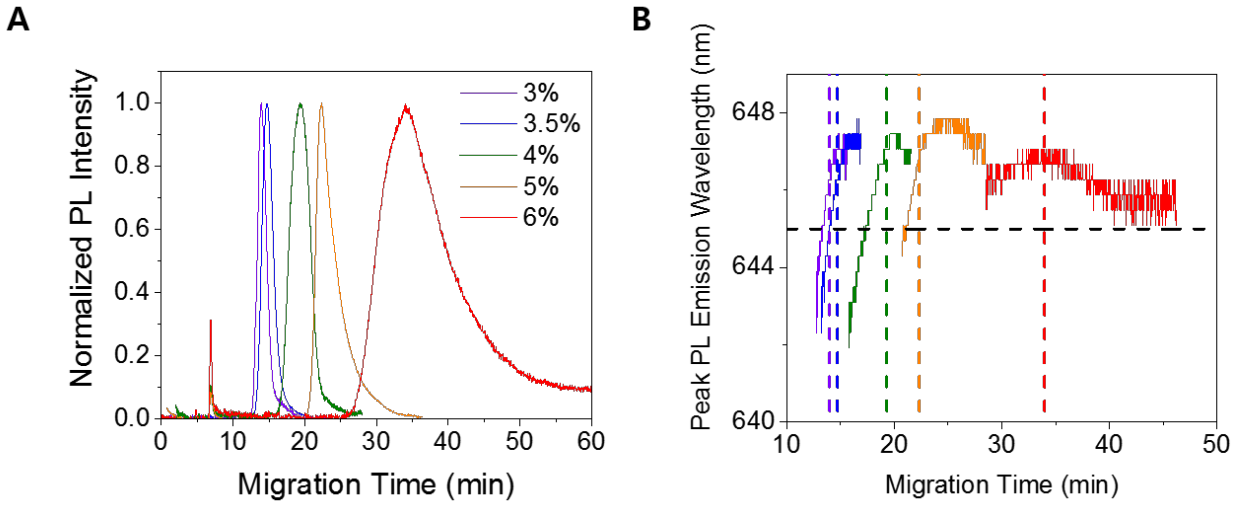

Fig. S4. (A) PL electropherograms of DHLA-SB-QD650 at different PAG densities. All other conditions were kept identical. **(B)** Corresponding changes in the peak PL emission wavelength over time. The horizontal dashed line is the wavelength of peak PL emission for the QDs in bulk solution. The vertical lines indicate the electropherogram peak positions.

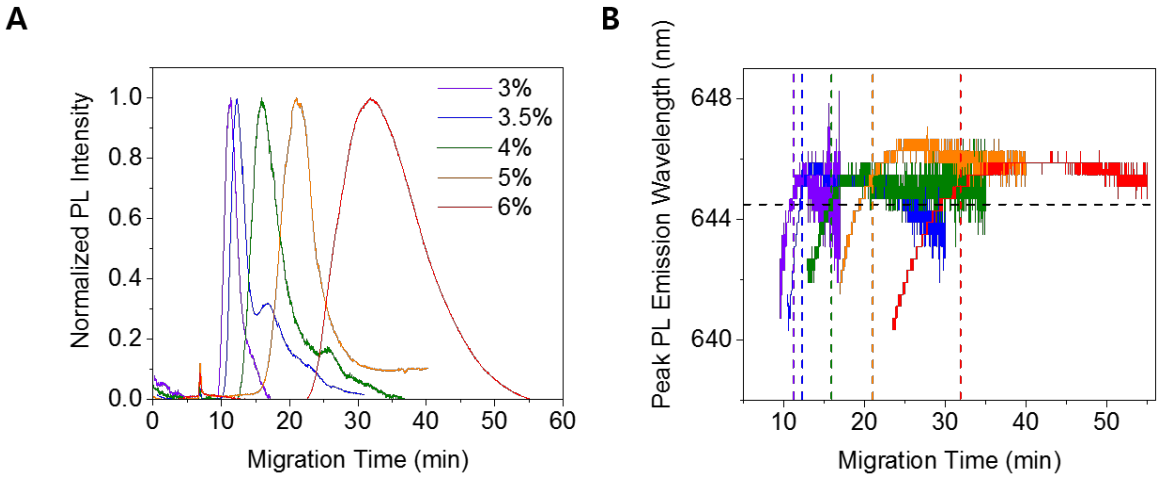

Fig. S5. (A) PL electropherograms of API-PMA-QD650 at different PAG densities. All other conditions were kept identical. **(B)** Corresponding changes in the peak PL emission wavelength over time. The horizontal dashed line is the wavelength of peak PL emission for the QDs in bulk solution. The vertical lines indicate the electropherogram peak positions.

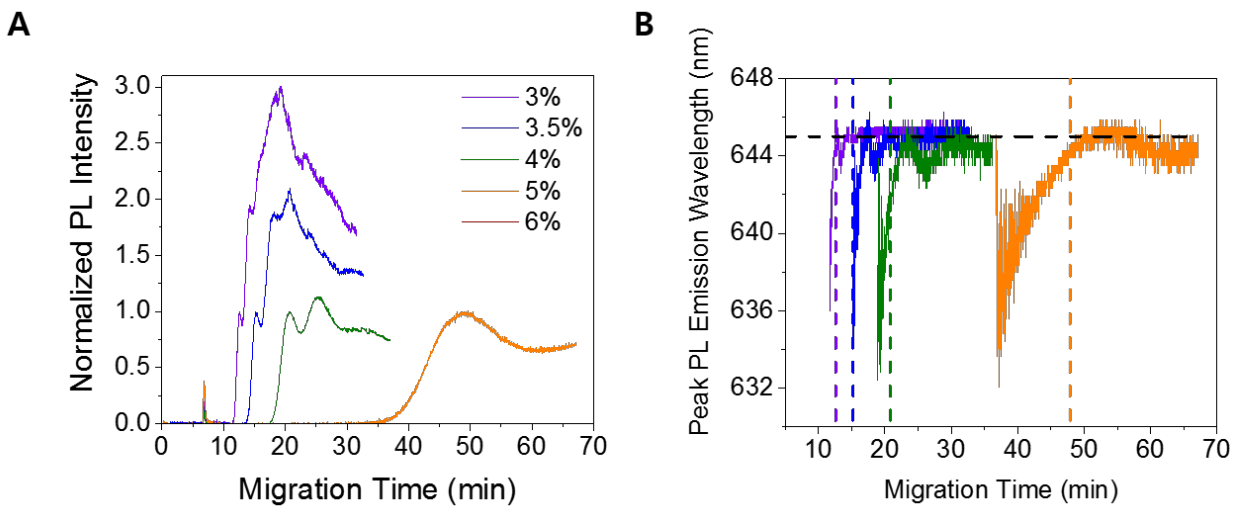

Fig. S6. (A) PL electropherograms of HDA-PMA-QD650 (batch 2) at different PAG densities. All other conditions were kept identical. **(B)** Corresponding changes in the peak PL emission wavelength over time. The horizontal dashed line is the wavelength of peak PL emission for the QDs in bulk solution. The vertical lines indicate the electropherogram peak positions for the first peak.

Shifts in QD PL emission spectra

Figs. S7–S9 (on the following three pages) show representative examples of the PL emission spectra of QD520, QD570, QD600, and QD650 at different points across their electropherogram peak, illustrating the observed spectral shift with migration time. In the case of the QD520 and, to a lesser extent, the QD570, the spectra measured over the electropherogram peak are shifted to significantly longer wavelengths than the ensemble PL spectrum measured in bulk solution. The reason is that the 530 nm cutoff for the longpass filter in the appartus is not sharp and attenuates the hypsochromic edge of each spectra, especially with the QD520. The result is an apparent but not real bathochromic shift in the position of the overall PL emission spectrum measured during the electropherogram. Nonetheless, the shifts in peak PL emission wavelength for QD520 and QD570 across their electropherogram peaks still reflect a real spectral shift with migration time, even if the absolute values of the maximum wavelength are not the real values.

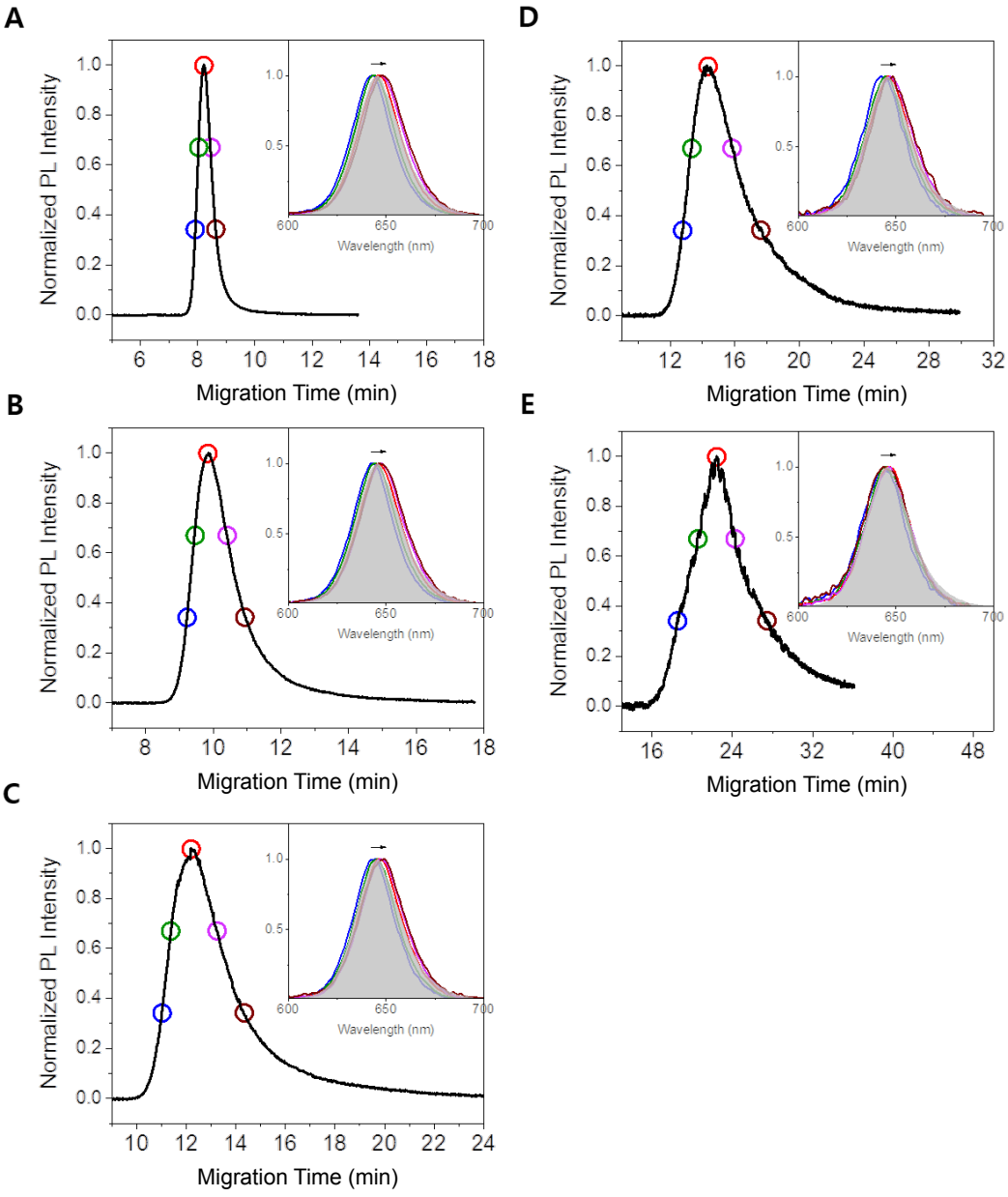

Fig. S7. PL electropherograms and examples of PL emission spectra (insets) measured at different points across the electropherogram peak for GSH-QD650. The solid grey spectrum is measured for the ensemble in bulk solution. **(A)** 3.0%, **(B)** 3.5%, **(C)** 4.0%, **(D)** 5.0%, and **(E)** 6.0% PAG gel densities.

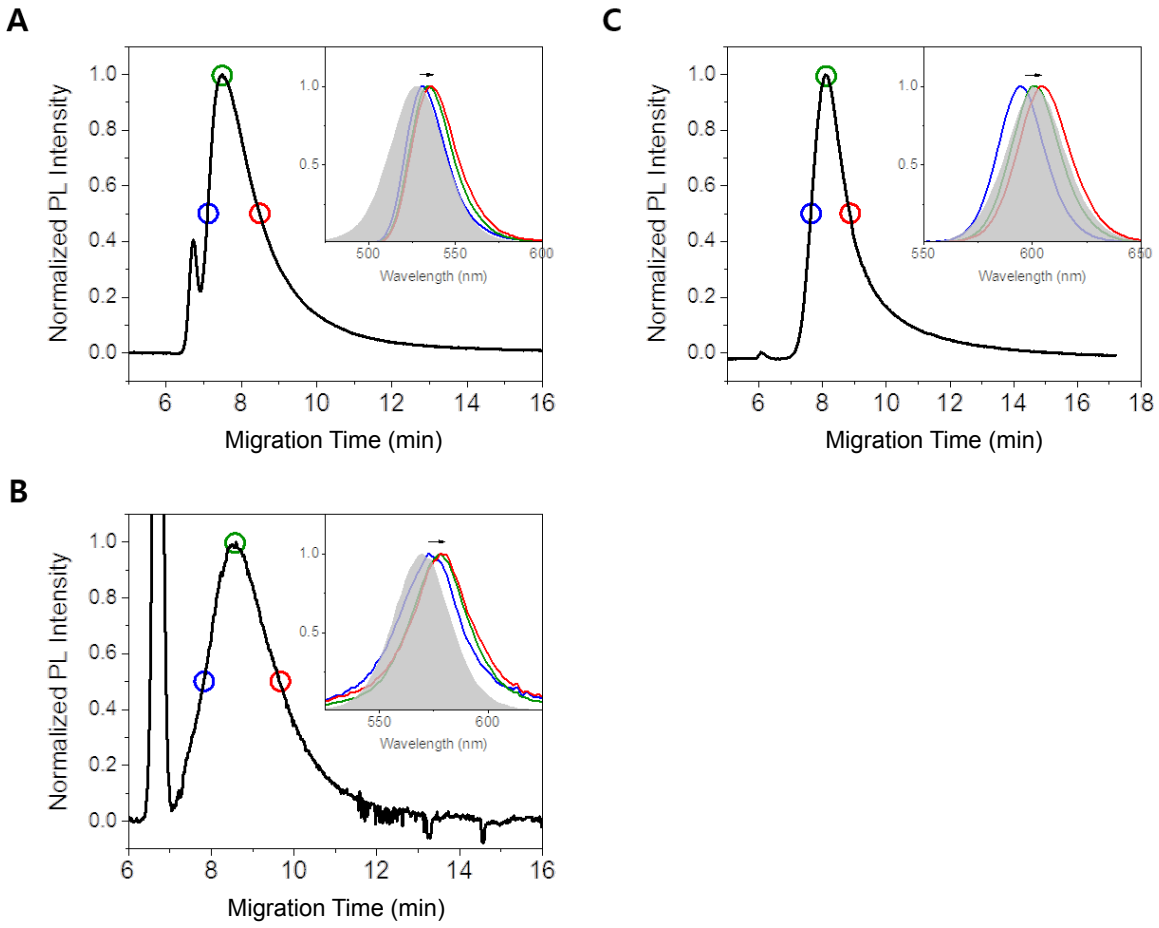

Fig. S8. PL electropherograms and examples of PL emission spectra (insets) measured at different points across the electropherogram peak for GSH-QDλ run in a 3.0% PAG. The solid grey spectrum is measured for the ensemble in bulk solution. **(A)** QD520, **(B)** QD570, and **(C)** QD600. Analogous data for QD650 is shown in Fig. 3.

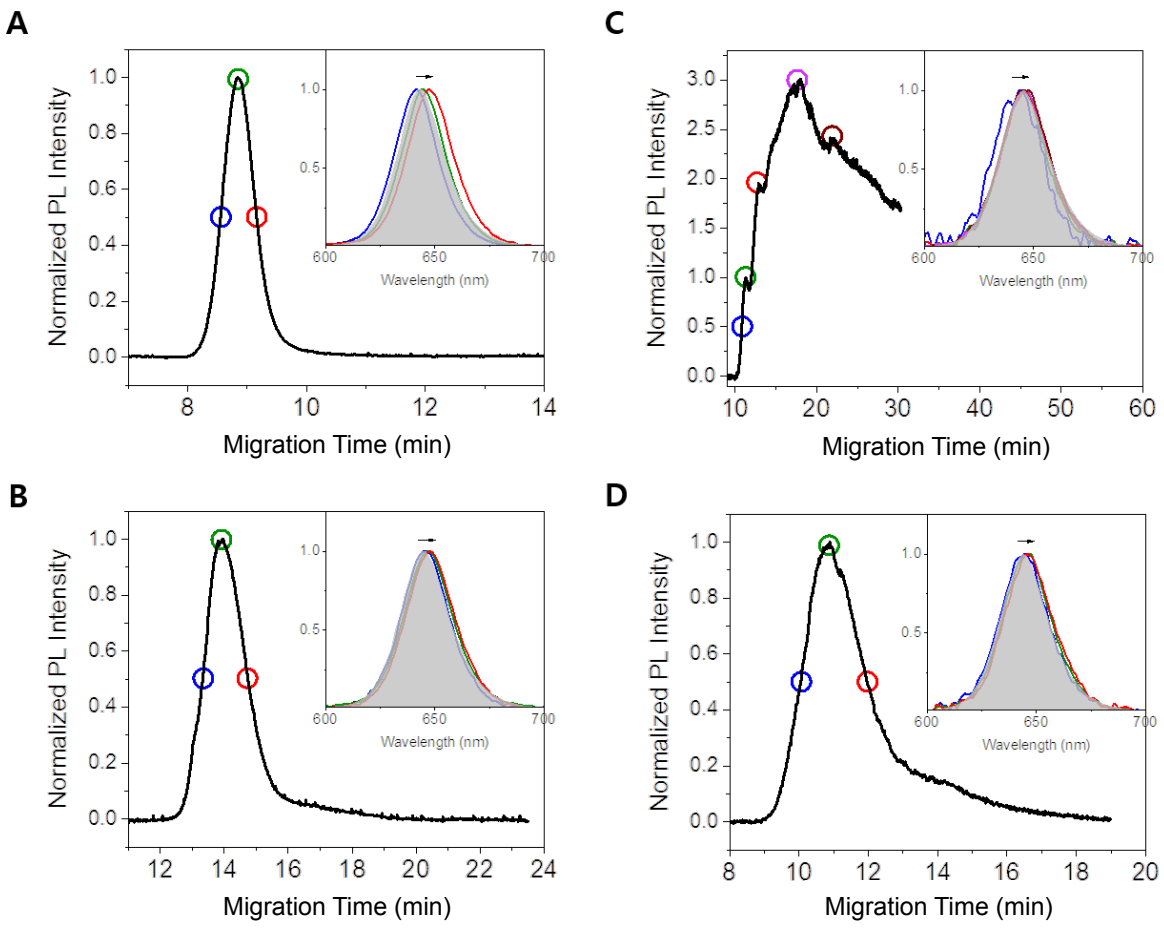

Fig. S9. PL electropherograms and examples of PL emission spectra (insets) measured at different points across the electropherogram peak for X-QD650 run on a 3.0% PAG. The solid grey spectrum is measured for the ensemble in bulk solution. X = **(A)** DHLA, **(B)** DHLA-SB, **(C)** HDA-PMA (batch 2), and **(D)** API-PMA. The spectrum in panel is normalized to the first peak rather than the overall maximum.

Wavelength shift and QD size

Fig. S10A shows the trend in the peak PL emission wavelength with migration time for GSH-QD650 and GSH-QD600 (reproduced from Fig. 3 and Fig. 6). The plots also show the relationship between the core radius and the predicted PL emission wavelength as per Eqn. S4. Fig. S10B shows the trend between QD size and inverse mobility, $1/M$, as per Eqn. S1, where $1/M$ is directly proportional to the migration time. The near linear trend (determination coefficients of 0.9998–0.9999) confirms that the bottom and top ordinates in Fig. S10A can be correlated as shown. There is good agreement between particle size, migration time, and peak PL emission wavelength over early portion of the electropherogram peaks for GSH-QD650 and GSH-QD600; however, the experimental data for migration time and peak PL emission wavelength negatively deviates from the prediction of Eqn. S4 over the late portion of the electropherogram peak. This result suggests a contribution to mobility other than size heterogeneity, likely in the form of charge heterogeneity from sub-populations of QDs with less than a saturating number of ligands, heterogeneity in shell thickness, or both.

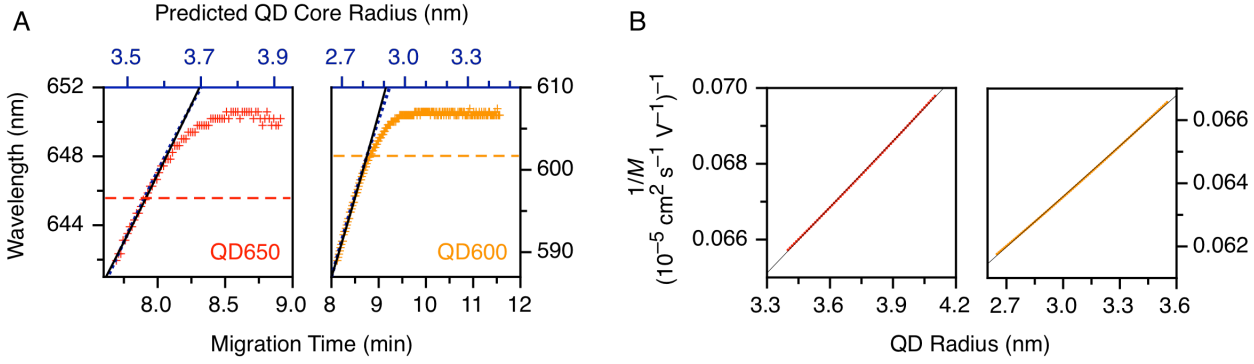

Fig. S10. (A) Plots of the experimentally measured peak PL emission wavelength versus migration time (bottom ordinate), and predicted PL emission wavelength versus QD core radius (top ordinate; blue line). The horizontal dashed line is the peak PL emission wavelength for the ensemble of QDs. **(B)** Plots of inverse mobility, $1/M$, versus QD radius, as per the Ferguson analysis. The data are fit with straight lines.

Analysis of QDs by CE

Several different QD materials were analyzed by capillary zone electrophoresis for a preliminary comparison to our "stubby" capillary PAGE format. The comparison was only partial as the available CE instrument was configured for diode array UV-visible absorption detection and not for spectral PL detection.

Fig. S11A shows electropherograms for the CZE of QD520, QD570, QD600, and QD650 coated with GSH ligands. The migration times scaled as QD520 < QD570 < QD650 ≈ QD600. This migration order was similar to the order for PAGE shown in Figure 4C. With PAGE, the different migration times were largely from differences in QD size; with CZE, the different migration times were from differences in net charge, which was presumed to be indirectly related to QD size via the number of bound ligands. The larger QD600 and QD650 had more bound charge and thus more electrophoretic mobility to oppose the electroosmotic flow (EOF). Notably, the bands in CZE were largely symmetric, in contrast to the tailing observed by PAGE. The band widths were qualitatively similar between CZE and PAGE, with the QD600 and QD650 having more narrow bands than the QD520 and QD570.

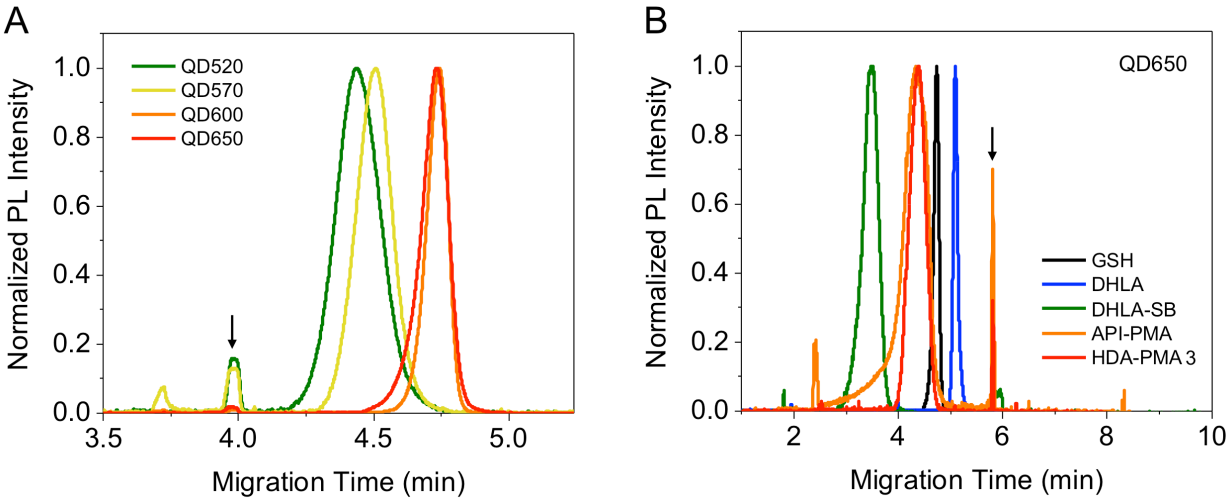

Fig. S11. CZE analysis of selected QD materials. **(A)** Electropherograms for QD520, QD570, QD600, and QD650 coated with GSH ligands. **(B)** Electropherograms for X-QD650, where X = GSH, DHLA, DHLA-SB, API-PMA, and HDA-PMA (batch 3). The arrows indicate peaks for the added internal standard: fluorescein in panel A and carboxyfluorescein in panel B.

Fig. S11B shows electropherograms for the CZE of X-QD650, where X = GSH, DHLA, DHLA-SB, API-PMA, and HDA-PMA (batch 3), the latter of which ran very similar to HDA-PMA-QD (batch 2) by PAGE. The migration times scaled as DHLA > GSH > API-PMA ≈ HDA-PMA > DHLA-SB. With the exception of GSH and DHLA, the order of migration times was a mirror image of those for PAGE (charge opposed the net mobility dominated by EOF in CE, whereas charge drove mobility in PAGE). CZE was able to distinguish between GSH-QD and DHLA-QD, unlike both agarose gels and PAGE. Relative peak widths were similar between CZE and PAGE, with more narrow peaks for GSH and DHLA and broader peaks for DHLA-SB, API-PMA, and HDA-PMA. A tail/front was observed with API-PMA-QD in both PAGE (Fig. 5B) and CZE; however, the CZE electropherogram was consistent with a homogeneous population of HDA-PMA-QD (batch 3) whereas PAGE (data not shown) indicated heterogeneity that was analogous to batch 2 in Fig. 5B. This contrast further suggested less size resolution in CZE than in PAGE. If spectral PL detection had been available with CZE, then greater insight into the balance of size versus charge effects in CZE and PAGE would have been possible.

Overall, the similarities between the trends with CZE and "stubby" capillary PAGE helped validate the latter method while the differences helped highlight its value as a characterization tool complementary to CZE, agarose gels, and other methods.

Analysis of gold nanoparticles by PAGE

To characterize gold nanoparticles (Au NPs), it was necessary to change the method of detection. Au NPs are not fluorescent but do scatter and absorb light strongly, which, in combination, is referred to as optical extinction. The detection method was therefore changed to a spectral extinction measurement using transmitted white light. The migrating band of Au NPs decreased the light intensity reaching the CCD spectrometer in accordance with its extinction spectrum, shown in Fig. S12A. The spectral detection feature is not as informative with Au NPs as it is with QDs because the optical properties of Au NPs change much less per unit change in size. Nonetheless, Fig. S12B shows that the "stubby" capillary PAGE method was able to resolve differences in the ligand coating (GSH versus DHLA) and size (5 nm versus 10 nm) between Au

NPs. There were differences in migration time between the two coatings and two sizes, as well as differences in electropherogram peak width between the two coatings.

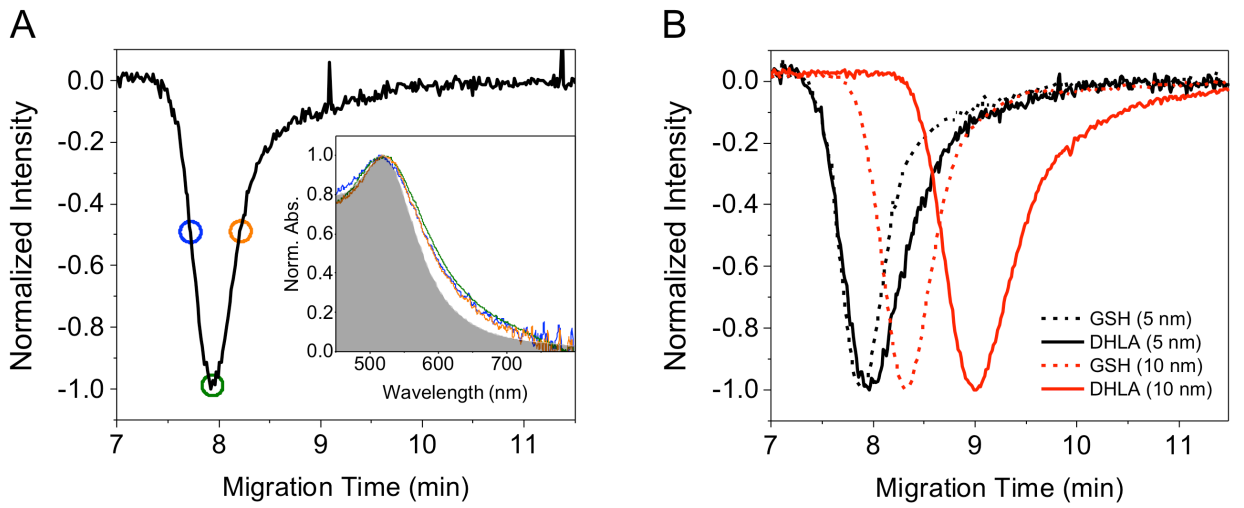

Fig. S12. (A) Comparison of the extinction spectra of Au NPs (5 nm, GSH coating) measured at three points across the electropherogram peak and versus the extinction spectrum for Au NPs in bulk solution (shaded). **(B)** Transmitted light electropherograms for GSH-Au NPs (5 nm, 10 nm) and DHLA-Au NPs (5 nm, 10 nm) with a 3.0% w/w PAG density.

Separation of fluorescent dye-labeled proteins by PAGE

Three fluorescent dye-labeled protein samples were prepared and analyzed by native PAGE in the "stubby" capillary format: BSA-FITC, BSA-RITC, and STI-FITC. The proteins were bovine serum albumin (BSA; 66 kDa, pI ~ 5) and soybean trypsin inhibitor (STI; 20 kDa, pI ~ 4.5). The dyes were the isothiocyanate derivatives of fluorescein (FITC) and Rhodamine B (RITC). Fig. S13 shows that the smaller STI-FITC had the highest mobility, followed by BSA-FITC and BSA-RITC. Resolution of the different mobilities of BSA-FITC and BSA-RITC was facilitated by the spectrofluorimetric detection. The BSA-RITC presumably had a lower mobility than the BSA-FITC because the RITC carried a positive charge whereas the FITC carried a negative charge.

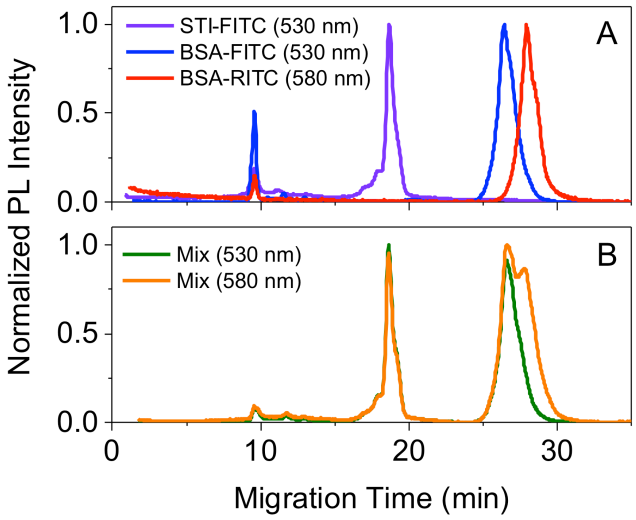

Fig. S13. (A) PL electropherograms for STI-FITC, BSA-FITC, and BSA-RITC, measured as individual samples. The electropherograms were plotted using the PL intensity at 530 nm for the STI-FITC and BSA-FITC, and using the PL intensity at 580 nm for BSA-RITC. **(B)** PL electropherograms plotted using the PL intensity measured at 530 nm and 580 nm for a mixture of all three labeled proteins. The PAGs were 7.5% w/w and run in borate buffer at pH 9.2.

Additional References

1. M. Wu, E. Petryayeva, I. L. Medintz and W. R. Algar, *Meth. Mol. Biol.*, 2014, **1199**, 215-239.
2. J. Park, J. Nam, N. Won, H. Jin, S. Jung, S. Jung, S. Cho and S. Kim, *Adv. Funct. Mater.*, 2011, **21**, 1558-1566.
3. T. Pons, H. T. Uyeda, I. L. Medintz and H. Mattoussi, *J. Phys. Chem. B*, 2006, **110**, 20308-20316.
4. S. Park, N. Sinha and K. Hamad-Schifferli, *Langmuir*, 2010, **26**, 13071-13075.
5. M. Wu and W. R. Algar, *ACS Appl. Mater. Inter.*, 2015, **7**, 2535-2545.
6. E. Petryayeva, T. Jeen and W. R. Algar, *ACS Appl. Mater. Inter.*, 2017, **9**, 30359-30372.
7. L. Brus, *J. Phys. Chem.*, 1986, **90**, 2555-2560.